

Detection of non separable correlations with dc transport: a new type of Aharonov-Bohm effect

R. Mélin*

Centre de Recherches sur les Très Basses Températures (CRTBT)[†]
CNRS BP 166X, 38042 Grenoble Cedex, France

November 23, 2018

Abstract

I construct a minimal formalism to describe transport of non separable correlations arising when a superconductor is in contact with several electrodes (being ferromagnetic or normal metal). Transport theory is expressed in terms of effective single site Green's functions. Part of the circuit is decimated exactly by renormalizing only one physical parameter (the density of states). I show that the physical current is obtained by acting on the infinite series of Feynman diagrams with an operator counting the charge of a given diagram. I use this method to propose a new Aharonov-Bohm experiment intended to detect non separable correlations. In this experiment, spin- σ electrons are forced to travel around an Aharonov-Bohm loop in the presence of an applied magnetic flux, while spin- $(-\sigma)$ electrons are not directly coupled to the magnetic flux. It is shown that the spin- $(-\sigma)$ current oscillates as a function of the flux to which spin- σ electrons are coupled. It is predicted that the effect exists both with high and low transparency contacts, and that the electrodes can be normal metal in which phase coherence can propagate over large distances. Three other aspects of the problem are investigated: (i) The dependence of the superconducting gap on spin polarization of ferromagnetic electrodes connected to the superconductor; (ii) The detection of linear superposition of correlated pairs of electrons; (iii) The proximity effect version of cryptomagnetism.

*melin@polycnrs-gre.fr

[†]U.P.R. 5001 du CNRS, Laboratoire conventionné avec l'Université Joseph Fourier

1 Introduction

There are two important challenges in phase coherent transport phenomena. One is to fabricate quantum bits for quantum computing [1, 2, 3, 4, 5, 6]. The other is to make an Einstein, Podolsky, Rosen (EPR) experiment, that would be able to probe Bell inequalities with electrons [7]. Bell inequalities have already been tested experimentally with photons [8, 9], being massless particles. EPR experiments constitute one of the ultimate tests of quantum mechanics, which is a non local theory without hidden variables (at least with photons). At the present stage, there exists no clear proposal of what should be an EPR experiment with electrons. It is not even known whether it is possible to propose a realistic situation in which a transport experiment could detect the presence/absence of hidden variables with electrons. However, electrons carry an electric charge while photons do not. One can take advantage of this, and propose experiments with electrons that would not be possible with photons.

It is already well established that the basic condition required to design an EPR experiment with electrons is to have a source of correlated pairs of electrons [5, 10]. Several dc transport experiments have been proposed recently [11, 12], and a new proposal is made here. From a technical point of view, I concentrate on the simplest non perturbative formulation of transport theory, which relies on the use of effective single site Green's functions. By non perturbative, I mean that transport theory is exact to all orders in the tunnel amplitude. As a consequence, I can solve the physics of high transparency contacts. The interesting aspect of the formalism is that part of the circuit can be decimated exactly. Only one physical parameter is renormalized (the density of states). I show how to cure a more technical problem, related to the fact that all possible Feynman diagrams are present in the theory and have exactly the same value. The solution is to act on the infinite series of Feynman diagrams with an operator counting the charge of a given diagram.

I apply the method to discuss four relevant physical questions:

- (i) What is the thermodynamics of a superconductor in the presence of correlated pairs of electrons ? I show that the strength of superconductivity depends on whether there exists or not non separable correlations in the vicinity of the superconductor. This may have direct implications for experiments.
- (ii) It is possible to fabricate linear superpositions of correlated pairs of electrons. How should one interpret transport of such states ? I show that transport theory is related to quantum measurement via projections of the linear superposition onto Cooper pair objects.
- (iii) Is there any way to manipulate one electron making the correlated pair and look at the response of the other electron ? I show that the answer is yes and propose a new type of Aharonov-Bohm effect that can be used to probe non separable correlations. Generically, there is no way to manipulate one electron without avoiding a response of the other electron.
- (iv) Is there a specific physics associated to Cooper pair penetration in ferromagnets in the presence of domain walls ? A simple model is solved, which shows that superconducting correlations can propagate along ferromagnetic domain walls. This may apply to recent experiments in ferromagnet – superconductor heterostructures [13, 14, 15], and constitutes the proximity version of cryptomagnetism.

Regarding the third question, it is worth recalling that in ordinary mesoscopic physics Aharonov-Bohm experiments [16, 17], electrons are forced to travel through a metallic ring in the presence of

a magnetic flux ϕ inside the hole of the ring. The current oscillates periodically as a function of ϕ , with a period equal to the flux quantum $\phi_0 = h/e$ [18]. This is because the system behaves like an interferometer in which the phase of the electronic wave function is related to the circulation of the vector potential. These oscillations occur in a variety of situations. For instance, the dual situation in which a magnetic flux is forced to travel around a magnetic charge is known as the Aharonov-Casher effect [19]. It is also very often that excitations of correlated states of matter do not carry a charge e . For instance, Cooper pairs carry a charge $2e$. The associated flux quantum is $h/(2e)$ [20]. Now when ferromagnetic or normal metal electrodes are connected to a superconductor, it is possible to fabricate correlated pairs of electrons of the type $c_{\alpha,\uparrow}^+ c_{\beta,\downarrow}^+ |0\rangle$ in which the spin-up and spin-down electrons making the Cooper pair reside in different electrodes. I propose here a situation in which the spin- σ electron making the Cooper pair is forced to couple to a vector potential (by propagating on a loop in the presence of a magnetic flux) while the spin- $(-\sigma)$ electron is not directly coupled to the magnetic flux (it propagates in an ordinary ferromagnet without any hole). As I show, *the spin- $(-\sigma)$ current oscillates as a function of the flux coupled to spin- σ electron*. This new type of Aharonov-Bohm effect can be viewed as a direct consequence of non separable correlations, and may be tested in future experiments.

The article is organized as follows. As a warm up exercise, I first calculate the transport formula associated to non local Andreev reflections in section 2. I introduce the effective single site formalism in section 3, and provide a discussion of higher order Feynman diagrams. Transport of linear superpositions of correlated pairs of electrons is derived in section 4. The Aharonov-Bohm experiment is discussed in section 5. I present in section 6 a simple model for superconducting propagation along a domain wall, which appears to be a problem closely related to non separable correlations. Final remarks are given in section 7.

2 Warming up: transport of non local Cooper pairs

I start by considering the model presented on Fig. 1 in which a superconductor is connected to N ferromagnetic electrodes. I first determine the superconducting gap in a self-consistent way, and next calculate the current I_n flowing into one of the ferromagnetic electrodes.

2.1 Effective single site Green's functions

Let us first describe the superconductor and ferromagnetic electrodes on the basis of effective single site Green's functions. The Nambu representation of the superconductor Green's function takes the form [21] $\hat{g}_{x,x}^{A,R}(\omega) = f\hat{I} + g\hat{\sigma}^x$, with

$$g(\omega \pm i\eta) = \pi\rho_N \frac{-\omega \pm i\eta}{\sqrt{\Delta^2 - (\omega \pm i\eta)^2}}, \text{ and } f(\omega \pm i\eta) = \pi\rho_N \frac{\Delta}{\sqrt{\Delta^2 - (\omega \pm i\eta)^2}},$$

where ρ_N is the normal density of states. The Nambu representation of the effective single site ferromagnetic Green's function reads $\hat{g}_{\alpha_k,\alpha_k}^{A,R} = \pm i\pi \left\{ \rho_{k,\uparrow}[\hat{I} + \hat{\sigma}^z]/2 + \rho_{k,\downarrow}[\hat{I} - \hat{\sigma}^z]/2 \right\}$, with $\rho_{k,\sigma}$ the spin- σ density of states in the ferromagnetic electrode α_k . The Nambu representation of the hopping matrix element is $\hat{t}_{x,\alpha_k} = t_{x,\alpha_k}\hat{\sigma}^z$. Using effective single site Green's functions means that the superconductor is viewed as being “zero dimensional”. This is a valid assumption if the distance between the contacts is smaller than the coherence length. This is precisely the condition under which non local Andreev reflections occur [12]. Therefore, representing the superconductor by effective single site Green's functions is a self consistent assumption.

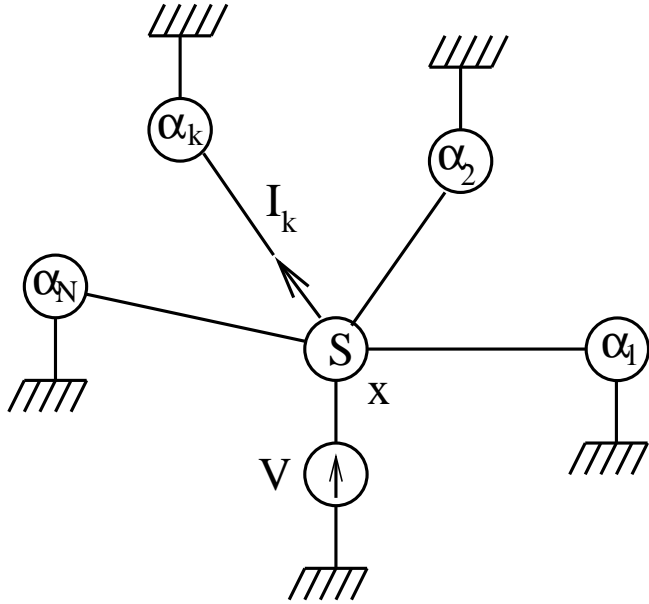


Figure 1: Schematic representation of the model considered in section 2 in which a superconductor (site x) is connected to N ferromagnetic electrodes (sites $\alpha_1, \dots, \alpha_N$). A voltage V is applied on the superconductor.

2.2 Self consistent determination of the superconducting gap

To determine the superconducting gap, we need to calculate the Gorkov function. First, we solve the Dyson equation

$$\hat{G}_{x,x}^{R,A} = \left[\hat{I} - \sum_{k=1}^N \hat{g}_{x,x}^{R,A} \hat{t}_{x,\alpha_k} \hat{g}_{\alpha_k,\alpha_k}^{R,A} \hat{t}_{\alpha_k,x} \right]^{-1} \hat{g}_{x,x}^{R,A}. \quad (1)$$

The relevant parameters appear to be the spectral line-width associated to spin- σ electrons: $\Gamma_\sigma = \sum_{k=1}^N \Gamma_{k,\sigma}$, with $\Gamma_{k,\sigma} = (t_{\alpha_k,x})^2 \rho_{k,\sigma}$. Solving Eq. 1 leads to

$$\hat{G}_{x,x}^A = \frac{1}{\mathcal{D}} \left\{ [g + i\pi(f^2 - g^2)] \hat{I} + f\hat{\sigma}^x \right\}, \quad (2)$$

with $\mathcal{D} = 1 - i\pi g(\Gamma_\uparrow + \Gamma_\downarrow) + \pi^2(f^2 - g^2)\Gamma_\uparrow\Gamma_\downarrow$. To calculate the superconducting order parameter, we need to solve the Dyson-Keldysh equation $\hat{G}^{+-} = (\hat{I} + \hat{G}^R \otimes \hat{W}) \otimes \hat{g}^{+-} \otimes (\hat{I} + \hat{W} \otimes \hat{G}^A)$, where the convolution includes a sum over the labels x and α_k . Noting $X_\sigma = (1 - i\pi g\Gamma_{-\sigma})/\mathcal{D}$, $Y_\sigma = i\pi f\Gamma_\sigma/\mathcal{D}$, and using Eq. 2, we obtain the exact expression of the Nambu component of the Keldysh Green's function:

$$\begin{aligned} [G_{x,x}^{+-}]_{2,1} &= 2i\pi n_F(\omega) \times \\ &\left\{ \rho_g (X_\uparrow \bar{Y}_\uparrow + Y_\downarrow \bar{X}_\downarrow) + \rho_f (X_\uparrow \bar{X}_\downarrow + Y_\downarrow \bar{Y}_\uparrow) \right. \\ &\left. + \frac{1}{\pi^2 \Gamma_\downarrow} \bar{Y}^\downarrow (X^\uparrow - 1) + \frac{1}{\pi^2 \Gamma^\uparrow} Y^\uparrow (\bar{X}^\downarrow - 1) \right\}, \end{aligned} \quad (3)$$

where $n_F(\omega)$ is the Fermi distribution, and I used the notation $\hat{\rho} = \rho_g \hat{I} + \rho_f \hat{\sigma}^x = \text{Im}[\hat{g}^A]/\pi$. The superconducting gap is obtained via the self-consistency equation [21]:

$$\Delta = U \int_{-\infty}^{+\infty} d\omega/(2i\pi) [\hat{G}^{+-}(\omega)]_{2,1},$$

with U the microscopic attractive interaction. The dominant contribution arises from the large- $|\omega|$ behavior, which leads to the BCS-type relation:

$$\Delta = D \exp \left[-\frac{1}{\rho_N U} (1 + \pi \rho_N \Gamma_\uparrow) (1 + \pi \rho_N \Gamma_\downarrow) \right], \quad (4)$$

with D the bandwidth of the superconductor. As an example, I consider a coupling to two ferromagnets. With a parallel alignment of the magnetizations in the electrodes, one has $\Gamma_\uparrow = 2\gamma$ and $\Gamma_\downarrow = 0$. With an antiparallel alignment, one has $\Gamma_\uparrow = \Gamma_\downarrow = \gamma$. The ratio of the two gaps is found to be

$$\frac{\Delta_{AP}}{\Delta_P} = \exp \left(-\frac{\pi^2 \rho_N \gamma^2}{U} \right) < 1, \quad (5)$$

which shows that the spin polarized environment generates a reduction of the superconducting gap, stronger with an antiferromagnetic alignment than with a ferromagnetic alignment. As a consequence, the transition temperature of the superconductor is larger if the electrodes are in a parallel alignment. This is valid whatever the transparency of the contacts.

To make contact with possible experiments, one should keep in mind the following points:

- (i) Eq. 5 should be strictly speaking applied only if the dimension of the superconductor is small compared to the coherence length.
- (ii) It is nevertheless possible to extrapolate to the physics occurring when a bulk superconductor is connected to ferromagnetic electrodes. In this case there is a non homogeneous gap in the superconductor, which is reduced at the interfaces with ferromagnetic electrodes. If two ferromagnetic electrodes are at a distance smaller than the coherence length, the *local* gap should follow *qualitatively* Eq. 5. A transport experiment involving two electrodes at a distance smaller than the coherence length would be sensitive to the *local* gap.

In the remaining of the article, I focus on transport properties. While keeping in mind that the superconducting gap should depend on the spin orientation of the ferromagnetic electrodes, I will not determine systematically the superconducting gap in a self consistent manner. Instead, I assume that the gap is a fixed quantity, but I could easily inject *a posteriori* the self consistent value of the gap in the transport equations.

2.3 Non local Andreev reflections

I use Green's function techniques to evaluate the current I_n flowing into the ferromagnetic electrode α_n as a trace over Nambu space:

$$I_n = \int d\omega \text{ Tr} \left\{ \left[\hat{t}_{\alpha_n, x} \hat{G}_{x, \alpha_n}^{+-}(\omega) - \hat{t}_{x, \alpha_n} \hat{G}_{\alpha_n, x}^{+-}(\omega) \right] \right\}. \quad (6)$$

Since it is trivial to restore the quantum of conductance in the transport formula, I assume that $e/h = 1$ throughout the article.

The Hamiltonian decomposes into two contributions:

$$\hat{\mathcal{H}} = \hat{\mathcal{H}}_x + \sum_{k=1}^N \hat{\mathcal{H}}_{\alpha_k} + \hat{\mathcal{W}},$$

where $\hat{\mathcal{H}}_x$ and $\hat{\mathcal{H}}_{\alpha_k}$ are associated to the superconducting and ferromagnetic electrodes, and $\hat{\mathcal{W}}$ is the coupling term:

$$\hat{\mathcal{W}} = \sum_{k=1}^N t_{\alpha_k, x} [c_{\alpha_k}^+ c_x + c_x^+ c_{\alpha_k}].$$

It is a standard method to treat $\hat{\mathcal{W}}$ as if it were a perturbation, and to sum to all orders the resulting perturbation theory. The final transport formula is then *non perturbative* in $\hat{\mathcal{W}}$ [22]. Therefore the method is well suited to describe the physics of high transparency contacts.

The chain of Dyson-Keldysh equations associated to Fig. 1 takes the form

$$\hat{t}_{x, \alpha_n} \hat{G}_{\alpha_n, x}^{+-} = \hat{t}_{x, \alpha_n} \sum_{k=1}^N \hat{G}_{\alpha_n, \alpha_k}^R \hat{t}_{\alpha_k, x} \hat{g}_{x, x}^{+-} \left[\hat{I} + \sum_{l=1}^N \hat{t}_{x, \alpha_l} \hat{G}_{\alpha_l, x}^A \right] \quad (7)$$

$$+ \hat{t}_{x, \alpha_n} \left[\hat{I} + \hat{G}_{\alpha_n, x}^R \hat{t}_{x, \alpha_n} \right] \hat{g}_{\alpha_n, \alpha_n}^{+-} \hat{t}_{\alpha_n, x} \hat{G}_{x, x}^A \quad (8)$$

$$+ \sum_{k \neq n} \hat{t}_{x, \alpha_n} \hat{G}_{\alpha_n, x}^R \hat{t}_{x, \alpha_k} \hat{g}_{\alpha_k, \alpha_k}^{+-} \hat{t}_{\alpha_k, x} \hat{G}_{x, x}^A. \quad (9)$$

The spin- σ Andreev current flowing into electrode α_n is found to be

$$I_{n, \sigma}^A = 4\pi^2 \Gamma_{n, \sigma} \Gamma_{-\sigma} \int d\omega [n_F(\omega - eV) - n_F(\omega)] |G_{x, x, 1, 2}^A|^2. \quad (10)$$

The Andreev current Eq. 10 is similar to the one of conventional Andreev reflection [21], except for the density of state prefactors appearing in the spectral line-widths. These prefactors reflect the fact that a spin- σ electron can be transferred in electrode α_n only if it paired with a spin- $(-\sigma)$ electron either in the same electrode (in which case the Cooper pair is a local object), or in another electrode (in which case a non local Cooper pair is transferred). This shows that the Andreev current is built up from a sum of all possible non local Cooper pair contributions, and generalizes the situation considered in Ref. [11].

3 Effective single site Green's functions formalism

Now I describe the method that will be used throughout the remaining of the article. The strategy is to use Green's functions techniques in an effective single site formalism. This method has proved to be extremely powerful in the context of superconducting quantum point contacts [21]. The advantage is that simple algebraic expressions can be manipulated without using spectral representations. The basic assumption is to consider that a given site represents a phase coherent continuum of states. I first take the example of the metal – metal – metal junction and show how to interpret the resulting transport theory. Since I consider in this section circuits without superconducting elements, the Nambu space structure is diagonal, and I can use spinless fermions without any loss of generality.

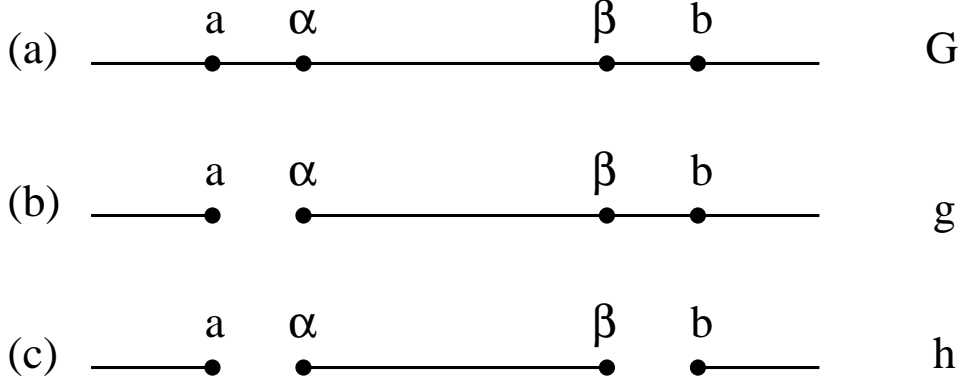


Figure 2: Notations for the Green's functions. In (a): no link is disconnected; the corresponding Green's functions are noted $G_{i,j}$. In (b): the link $a - \alpha$ is disconnected; the corresponding Green's functions are noted $g_{i,j}$. In (c): The two links $a - \alpha$ and $b - \beta$ are disconnected. The Green's functions are noted $h_{i,j}$. One has $g_{a,a} = h_{a,a}$.

3.1 Treating all couplings on the same footing

Let us start to calculate the transport formula corresponding to the metal – metal – metal junction shown on Fig. 2. We note G the Green's function of the fully connected system, g the Green's function with $t_{a,\alpha} = 0$, and h the Green's function with $t_{a,\alpha} = t_{b,\beta} = 0$ (see Fig. 2).

I treat simultaneously the two couplings $t_{a,\alpha}$ and $t_{b,\beta}$ on the same footing. Namely, I go directly from the G 's to the h 's without ever using the g 's. The chain of Dyson equations for the Green's function takes the form

$$G_{a,a} = h_{a,a} + h_{a,a}t_{a,\alpha}h_{\alpha,\alpha}t_{\alpha,a}G_{a,a} + h_{a,a}t_{a,\alpha}h_{\alpha,\beta}t_{\beta,b}G_{b,a} \quad (11)$$

$$G_{b,a} = h_{b,b}t_{b,\beta}h_{\beta,\beta}t_{\beta,b}G_{b,a} + h_{b,b}t_{b,\beta}h_{\beta,\alpha}t_{\alpha,a}G_{a,a}. \quad (12)$$

The effective single site Green's functions are $h_{a,a}^{A,R} = \pm i\pi\rho_a$, $h_{i,j}^{A,R} = \pm i\pi\rho$ ($i, j = \alpha, \beta$), $h_{b,b}^{A,R} = \pm i\pi\rho_b$. I use the notation $\gamma_a = \pi^2|t_{a,\alpha}|^2\rho_a$ and $\gamma_b = \pi^2|t_{b,\beta}|^2\rho_b$. Eqs. 11 – 12 are solved in a straightforward fashion. For instance, one obtains

$$G_{a,a}^{A,R} = \pm i\pi\rho_a \frac{1 + \rho\gamma_b}{1 + \rho(\gamma_a + \gamma_b)}.$$

Next, I calculate the Keldysh component

$$G_{a,\alpha}^{+-} = [1 + G_{a,\alpha}^R T_{\alpha,a}] h_{a,a}^{+-} t_{a,\alpha} G_{\alpha,\alpha}^A + G_{a,a}^R t_{a,\alpha} h_{\alpha,\alpha}^{+-} [1 + t_{\alpha,a} G_{a,\alpha}^A] + G_{a,a}^R t_{a,\alpha} h_{\alpha,\beta}^{+-} t_{\beta,b} G_{b,\alpha}^A \quad (13)$$

$$+ G_{a,b}^R t_{b,\beta} h_{\beta,\alpha}^{+-} [1 + t_{\alpha,a} G_{a,\alpha}^A] + G_{a,b}^R t_{b,\beta} h_{\beta,\beta}^{+-} t_{\beta,b} G_{b,\alpha}^A + G_{a,\beta}^R t_{\beta,b} h_{b,b}^{+-} t_{b,\beta} G_{\beta,\alpha}^A. \quad (14)$$

It is straightforward to evaluate the six terms to obtain the transport formula

$$I_{a,\alpha} = \int d\omega \frac{2\rho\gamma_a(1 + \rho\gamma_b)}{[1 + \rho(\gamma_a + \gamma_b)]^2} [n_F(\omega - eV) - n_F(\omega)]. \quad (15)$$

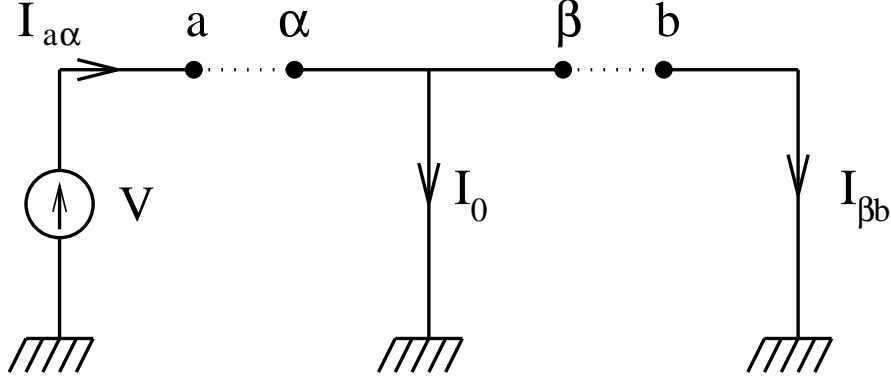


Figure 3: Representation of the current flow. I_0 is a disconnected current and only $I_{\beta,b}$ is relevant.

3.2 Decimating part of the circuit

Before discussing the physics of Eq. 15, I give another derivation of this transport formula. The idea is to use first a perturbation in $t_{b,\beta}$ and, in a second step, make a perturbation in $t_{a,\alpha}$. Namely, part of the circuit is decimated exactly, and I look for an effective theory for the remaining sites.

The perturbation in $t_{a,\alpha}$ leads to

$$G_{a,\alpha}^{+-} = G_{a,a}^R t_{a,\alpha} g_{\alpha,\alpha}^{+-} [1 + t_{\alpha,a} G_{a,\alpha}^A] + [1 + G_{a,\alpha}^R t_{\alpha,a}] g_{a,a}^{+-} t_{a,\alpha} G_{\alpha,\alpha}^A. \quad (16)$$

Therefore, I need to determine $g_{\alpha,\alpha}^{+-}$ and $g_{a,a}^{+-}$ in terms of the h 's. The chain of Dyson equations reads

$$g_{\alpha,\alpha} = h_{\alpha,\alpha} + h_{\alpha,\beta} t_{\beta,b} g_{b,\alpha} \quad (17)$$

$$g_{b,\alpha} = h_{b,b} t_{b,\beta} g_{\beta,\alpha} \quad (18)$$

$$g_{\beta,\alpha} = h_{\beta,\alpha} + h_{\beta,\beta} t_{\beta,b} g_{b,\alpha}. \quad (19)$$

The equation for the Keldysh component is

$$g_{\alpha,\alpha}^{+-} = g_{\alpha,b}^R t_{b,\beta} h_{\beta,\beta}^{+-} t_{\beta,b} g_{b,\alpha}^A + h_{\alpha,\alpha}^{+-} + h_{\alpha,\beta}^{+-} t_{\beta,b} g_{b,\alpha}^A + g_{\alpha,b}^R t_{b,\beta} h_{\beta,\alpha}^{+-} + g_{\alpha,\beta}^R t_{\beta,b} h_{b,b}^{+-} t_{b,\beta} g_{\beta,\alpha}^A. \quad (20)$$

It is straightforward to solve Eqs. 17 – 20, inject the propagators into Eq. 16 and find the current Eq. 15. In this approach, the effect of the coupling β – b is just to renormalize the density of states at site α : $g_{\alpha,\alpha}^{+-} = 2i\pi n_F(\omega) \tilde{\rho}_\alpha$, $g_{\alpha,\alpha}^{A,R} = \pm i\pi \tilde{\rho}_\alpha$, with

$$\tilde{\rho}_\alpha = \frac{\rho}{1 + \rho \gamma_b}, \quad (21)$$

where ρ is the density of states in the intermediate region and $\gamma_b = \pi^2 |t_{b,\beta}|^2 \rho_b$. We will apply this decimation method latter in more complicated situations.

3.3 Interpretation of the transport formula

The current Eq. 15 can be decomposed into two contributions: $I_{a,\alpha} = I_0 + I_{\beta,b}$, with

$$I_0 = \int d\omega \frac{2\rho \gamma_a}{[1 + \rho(\gamma_a + \gamma_b)]^2} [n_F(\omega - eV) - n_F(\omega)], \quad (22)$$

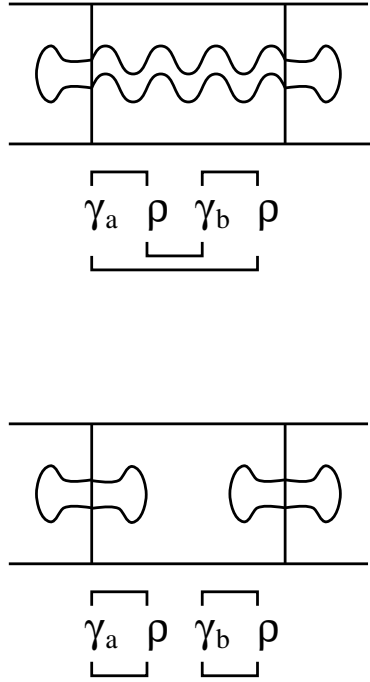


Figure 4: The diagrams of order $\rho^2\gamma_a\gamma_b$ contributing to $I_{\beta,b}$. The top diagram has a unit charge ($Q = 1$). The bottom diagram has a zero charge ($Q = 0$).

and

$$I_{\beta,b} = \int d\omega \frac{2\rho^2\gamma_a\gamma_b}{[1 + \rho(\gamma_a + \gamma_b)]^2} [n_F(\omega - eV) - n_F(\omega)]. \quad (23)$$

It is straightforward to calculate directly the current flowing through the link $\beta - b$, and show that it coincides with Eq. 23. Therefore, we are lead to consider that the region $\alpha - \beta$ can absorb part of the electrical current (see Fig. 3). Only is the transmitted current $I_{\beta,b}$ a quantity of interest. To understand the appearance of the fake term I_0 , it is useful to notice that an effective single site plays two roles at the same time:

- (i) It transmits current to the rest of the circuit. This is why there is a finite contribution $I_{\beta,b}$.
- (ii) It represents a continuum of energy levels; therefore, it also plays by itself the role of a reservoir. This is why there is a finite current I_0 .

Now the expression (23) of $I_{\beta,b}$ contains also a renormalization prefactor which generates an infinite series of Feynman diagrams. It turns out that disconnected contributions are also present in these diagrams. To obtain the final form of the physical current, we expand Eq. 23 in an infinite series of Feynman diagrams, and operate on this series with an operator \hat{Q} that multiplies each Feynman diagram its charge:

$$I_{\text{phys}} = \int d\omega \hat{Q} \left[\frac{2\rho^2\gamma_a\gamma_b}{[1 + \rho(\gamma_a + \gamma_b)]^2} \right] [n_F(\omega - eV) - n_F(\omega)]. \quad (24)$$

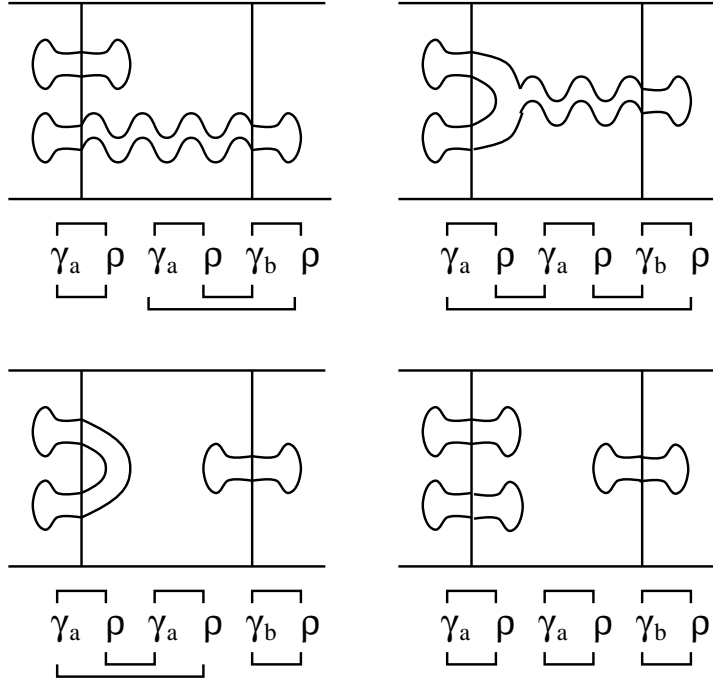


Figure 5: The four diagram of order $\rho^3 \gamma_a^2 \gamma_b$ contributing to $I_{\beta,b}$. The two top diagrams has a unit charge ($Q = 1$). The two bottom diagrams have a zero charge ($Q = 0$).

In the case of the metal – metal – metal junction, Eq. 24 should coincide with the transport formula obtained by Caroli *et al.* [22]:

$$I_{\text{phys}} = \int d\omega \frac{\rho^2 \gamma_a \gamma_b}{[1 + \rho(\gamma_a + \gamma_b)]^2} [n_F(\omega - eV) - n_F(\omega)]. \quad (25)$$

To verify this, I calculate the lowest order diagrams associated to Eq. 24. This will give us the opportunity to show how the operator \hat{Q} operates.

3.4 Feynman diagrams

To count how many diagrams appear at a given order, we expand Eq. 23 in a power series:

$$\frac{2\rho^2 \gamma_a \gamma_b}{(1 + \rho(\gamma_a + \gamma_b))^2} = 2\rho^2 \gamma_a \gamma_b - 4\rho^3 \gamma_a \gamma_b (\gamma_a + \gamma_b) + 6\rho^4 \gamma_a \gamma_b (\gamma_a + \gamma_b)^2 + \dots \quad (26)$$

From what we deduce that there are two diagrams at order $\gamma_a \gamma_b$, four diagrams at order $\gamma_a^2 \gamma_b$, six diagrams at order $\gamma_a^3 \gamma_b$, twelve diagrams at order $\gamma_a^2 \gamma_b^2$, etc ... Each of the diagrams corresponds to a possible contraction of the density of states. For instance the two diagrams at order $\gamma_a \gamma_b$ are shown on Fig. 4. The four diagrams at order $\gamma_a^2 \gamma_b$ are shown on Fig. 5. The twelve diagrams at order $\gamma_a^2 \gamma_b^2$ are shown on Fig. 6. Using these diagrams to evaluate Eq. 24, we obtain the expansion

$$I_{\text{phys}} = \int d\omega [\rho^2 \gamma_a \gamma_b - 2\rho^3 \gamma_a \gamma_b (\gamma_a + \gamma_b) + 3\rho^4 \gamma_a \gamma_b (\gamma_a + \gamma_b)^3 + \dots] \times [n_F(\omega - eV) - n_F(\omega)],$$

which coincides with the expansion of Eq. 25.

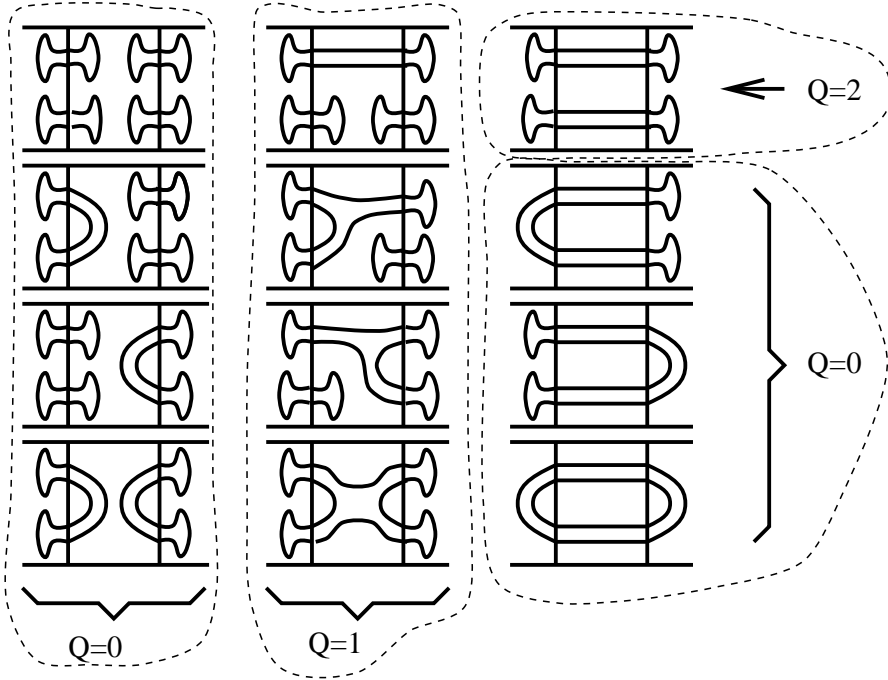


Figure 6: The twelve diagram of order $\rho^4 \gamma_a^2 \gamma_b^2$ contributing to $I_{\beta,b}$. The charges are indicated.

4 Transport of linear superposition of correlated pairs

4.1 EPR paradox

It is worth recalling the well known EPR paradox [23]. Let us consider a collision of two spin-1/2 electrons. The collision is represented by an antiferromagnetic exchange interaction $J(\tau) \mathbf{S}_1 \cdot \mathbf{S}_2$, where $J(\tau)$ is constant in the time interval $[0, t]$ and zero otherwise. After the collision, the system is represented by the EPR state

$$|\psi\rangle = \cos(\Omega t)|+-\rangle - i \sin(\Omega t)|-+\rangle, \quad (27)$$

with $\Omega = J/2$. Let us imagine that two observers \mathcal{O}_1 and \mathcal{O}_2 use an apparatus (i.e. a Stern and Gerlach magnet) to measure the spin orientation of \mathbf{S}_1 and \mathbf{S}_2 . The observer \mathcal{O}_1 measuring S_1^z would find 1/2 with a probability $\cos^2(\Omega t)$ and -1/2 with a probability $\sin^2(\Omega t)$. Once the observer \mathcal{O}_1 has made his measurement, the wave function collapses and with a probability one, the observer \mathcal{O}_2 measuring S_2^z would find $S_2^z = 1/2$ if \mathcal{O}_1 has measured $S_1^z = -1/2$, and $S_2^z = -1/2$ if \mathcal{O}_1 has measured $S_1^z = 1/2$. Quantum mechanics contains non separable correlations, which is the famous EPR paradox [23]. As pointed out by Bell, there exists a basic difference between quantum mechanics and hidden variable theories [7]. It has been demonstrated experimentally that Bell inequalities were violated with photons [8, 9], therefore ruling out hidden variable theories (at least with photons). As already mentioned in the Introduction, it is an open question to test the EPR paradox with electrons. We do not address this issue directly in this article. Nevertheless, we find an interesting connection between transport properties and quantum measurement (i.e. projections) of linear superpositions of correlated pairs.

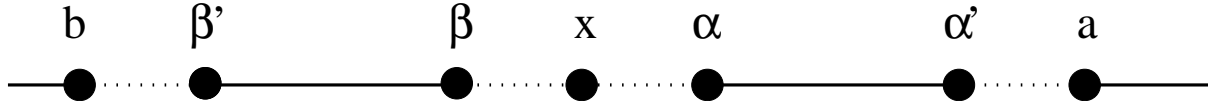


Figure 7: Schematic representation of the model considered in section 4. The site x is superconducting. The intermediate regions $\alpha - \alpha'$ and $\beta - \beta'$ are ferromagnetic. The electrodes a and b are ferromagnetic.

4.2 Fabrication of linear superpositions of correlated pairs

Now I use the formalism presented in section 3 to discuss the physics of linear superpositions of correlated pairs of electrons. I consider that a ballistic ferromagnetic region $\alpha_k - \alpha'_k$ is inserted in between the superconducting site x and the external ferromagnetic electrodes a_k (see Figs. 7 and 8).

To simplify the discussion, I make the following assumptions:

- (i) There are no pair correlations between the bottom electrode on Fig. 7 (used to impose the superconductor chemical potential) and the other ferromagnetic electrodes. This means that the corresponding contact on the superconductor is separated from the other contacts by a distance much larger than the superconducting coherence length.
- (ii) All ferromagnets are fully polarized. Therefore, there is no transmission of local Cooper pairs.
- (iii) The ferromagnetic intermediate regions are phase coherent. Present time technology does not allow the fabrication of such devices. Nevertheless, the model is interesting *per se*.

Our analysis of the situations presented on Figs. 7 and 8 is the following. The wave function in the ballistic regions is a linear superposition of correlated pairs. For instance, in the presence of three fully polarized ferromagnetic regions connected to the superconductor having a spin orientation $\sigma_\alpha = \uparrow$, $\sigma_\beta = \sigma_\gamma = \downarrow$ (see Fig. 8), the wave function is

$$|\psi\rangle = c_{\alpha,\uparrow}^+ \left[\sqrt{\frac{t_\beta \rho_{\beta,\downarrow}}{t_\beta \rho_{\beta,\downarrow} + t_\gamma \rho_{\gamma,\downarrow}}} c_{\beta,\downarrow}^+ + \sqrt{\frac{t_\gamma \rho_{\gamma,\downarrow}}{t_\beta \rho_{\beta,\downarrow} + t_\gamma \rho_{\gamma,\downarrow}}} c_{\gamma,\downarrow}^+ \right] |0\rangle. \quad (28)$$

In the presence of spin orientations $\sigma_\alpha = \sigma_\beta = \uparrow$, $\sigma_\gamma = \downarrow$, we have

$$|\psi'\rangle = \left[\sqrt{\frac{t_\beta \rho_{\beta,\uparrow}}{t_\alpha \rho_{\alpha,\uparrow} + t_\beta \rho_{\beta,\uparrow}}} c_{\beta,\uparrow}^+ + \sqrt{\frac{t_\alpha \rho_{\alpha,\uparrow}}{t_\alpha \rho_{\alpha,\uparrow} + t_\beta \rho_{\beta,\uparrow}}} c_{\alpha,\uparrow}^+ \right] c_{\gamma,\downarrow}^+ |0\rangle. \quad (29)$$

These wave functions are the only ones that can guarantee the correct pairing associated to the formation of correlated pairs of electrons. The coefficients of the wave function can be obtained by evaluating the Gorkov function. With the configuration $\sigma_\alpha = \sigma_\beta = \uparrow$, $\sigma_\gamma = \downarrow$, we find

$$\left[\hat{G}_{\alpha(\beta),\gamma}^{+-} \right]_{1,2} = \pi^2 t_{\alpha(\beta)} t_\gamma \rho_{\alpha(\beta),\uparrow} \rho_{\gamma,\downarrow} \left[\hat{G}_{x,x}^{+-} \right]_{1,2}.$$

From what we deduce Eq. 28. We will come back in section 4.4 on the meaning of this wave function.

The dictionary between the Cooper pair wave function Eq. 28 and the spin-1/2 wave function Eq. 27 is the following:

$$| + - \rangle \leftrightarrow c_{\alpha,\uparrow}^+ c_{\beta,\downarrow}^+ \quad (30)$$

$$| - + \rangle \leftrightarrow c_{\alpha,\uparrow}^+ c_{\gamma,\downarrow}^+. \quad (31)$$

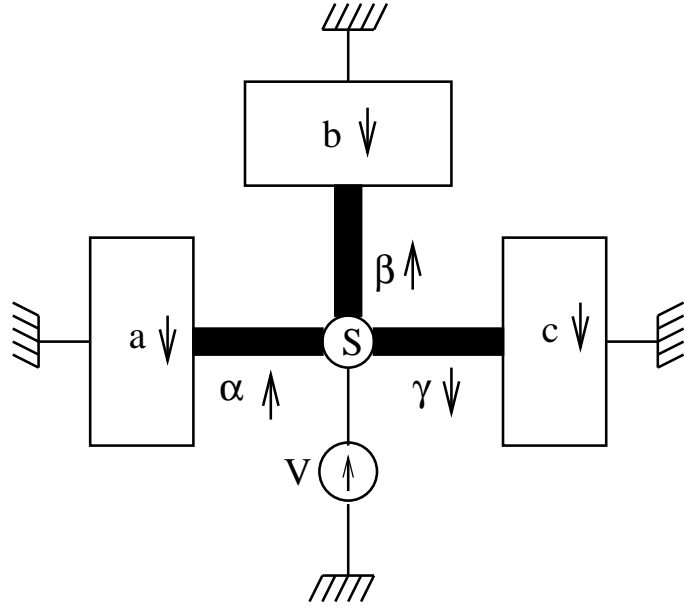


Figure 8: Representation of a device in which three ferromagnetic electrodes α, β, γ are connected to a superconductor. The additional electrodes a, b, c are used to perform a measurement of the linear superposition of correlated pairs.

The relevant question that should be asked now is to determine whether it is possible to make a quantum measurement of the linear superposition of correlated pairs, similar to the Stern and Gerlach measurement of the spin-1/2 EPR state. Namely, we want to interpret transport theory in terms of projection operators.

4.3 Transport formula

The strategy to solve the model on Fig. 7 within the effective single site Green's function approach is to use the two step perturbation theory presented in section 3.2. I first treat the link $\alpha' - a$ in perturbation (see Fig. 7). Since the superconducting site has been disconnected and there is no source of spin flip scattering, the Dyson equations decouple into a spin-up and a spin-down component. We note $h_{i,j}$ the Green's functions of the disconnected system, *i.e.* with $t_{a,\alpha_k} = 0$. The Dyson equation for the Keldysh component has already been given in section 3. The solution takes the form $g_{\alpha,\alpha,\sigma}^{+-} = 2i\pi n_F(\omega)\tilde{\rho}_{\alpha,\sigma}$, and $g_{\alpha,\alpha,\sigma}^{A,R} = \pm i\pi\tilde{\rho}_{\alpha,\sigma}$, with the renormalized density of states

$$\tilde{\rho}_{\alpha,\sigma} = \frac{\rho_{\alpha,\sigma}}{1 + \pi^2|t_{a,\alpha}|^2\rho_{\alpha,\sigma}\rho_{a,\sigma}}.$$

Next, I use a perturbation in t_{x,α_k} to calculate the Andreev current. This is done by noticing that the physical current $I_{\alpha,a}$ is a finite fraction of the current incoming at site α (see Eqs. 22, 23):

$$\frac{I_{\alpha,a}}{I_{x,\alpha}} = \frac{\pi^2|t_{a,\alpha}|^2\rho_a\rho_\alpha}{1 + \pi^2|t_{a,\alpha}|^2\rho_a\rho_\alpha}. \quad (32)$$

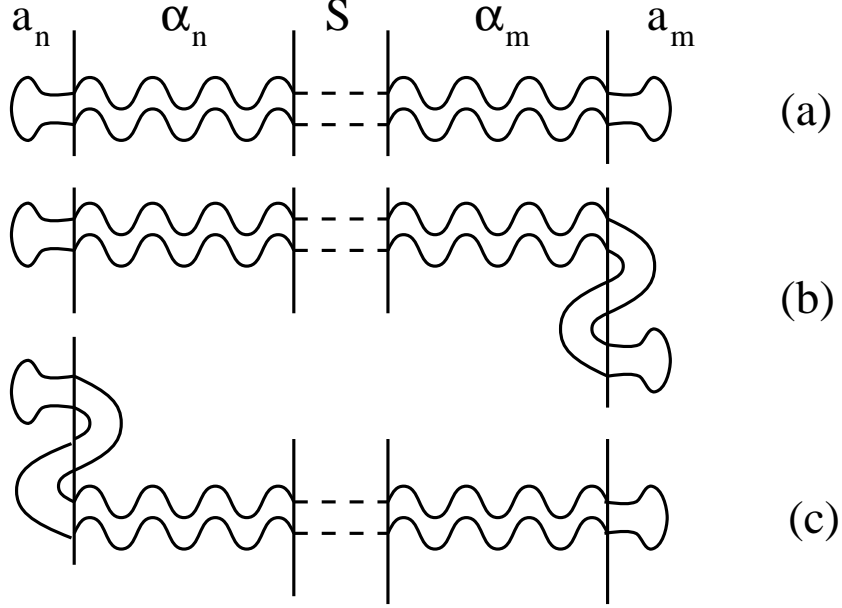


Figure 9: The relevant lowest order Andreev reflection diagrams. (a) is of order $\rho_{a_n}\rho_{a_m}(\rho_{\alpha_n})^2(\rho_{\alpha_m})^2$. (b) is of order $\rho_{a_n}(\rho_{a_m})^3(\rho_{\alpha_n})^2(\rho_{\alpha_m})^4$. (c) is of order $(\rho_{a_n})^3\rho_{a_m}(\rho_{\alpha_n})^4(\rho_{\alpha_m})^2$. The dashed line represents the anomalous propagation in the superconductor.

I deduce from Eq. 32 that the Andreev current Eq. 10 is the sum of all possible Cooper pair transmissions:

$$I_{n,\sigma}^A = 4\pi^2 \int d\omega [n_F(\omega - eV) - n_F(\omega)] \sum_m \hat{Q} [u_{n,\sigma,\sigma'} u_{m,-\sigma,\sigma'}] |G_{x,x,1,2}^A|^2, \quad (33)$$

where

$$u_{n,\sigma,\sigma'} = \pi^2 |t_{x,\alpha_n}|^2 |t_{a_n,\alpha_n}|^2 \frac{\rho_{\alpha_n,\sigma}^2 \rho_{a_n,\sigma}}{(1 + \pi^2 |t_{a_n,\alpha_n'}|^2 \rho_{\alpha_n,\sigma} \rho_{a_n,\sigma})^2}. \quad (34)$$

The action of \hat{Q} in Eq. 33 has already been given. The form Eq. 33 of the current can also be obtained by making directly a perturbation in t_{x,α_k} to evaluate the current through the link $\alpha_n - a_n$. The density of state prefactors appearing in the lowest contribution in Eq. 33 corresponds to the diagram on Fig. 9 (a).

4.4 Quantum measurement of the superposition of correlated pairs

Let us now interpret the transport formula Eq. 33 in terms of quantum measurement of the superposition of correlated pairs. We assume that the external ferromagnetic electrodes are weakly coupled to the intermediate regions. As a consequence, we make the approximation $\tilde{\rho}_\alpha = \rho_\alpha$. The interfaces with the superconductor can be either tunnel or high transparency contacts. The general form of the linear superposition is

$$|\psi\rangle = \mathcal{N}^{-1/2} \sum_{p,q} \sqrt{t_{\alpha_p} t_{\alpha_q} \rho_{\alpha_p,\uparrow} \rho_{\alpha_q,\downarrow}} c_{\alpha_p,\uparrow}^+ c_{\alpha_q,\downarrow}^+ |0\rangle, \quad (35)$$

where

$$\mathcal{N} = \sum_p t_{\alpha_p} \rho_{\alpha_p, \uparrow} \sum_q t_{\alpha_q} \rho_{\alpha_q, \downarrow}.$$

It is useful to define a projection operator associated to the correlated pairs of electrons ($p \uparrow, q \downarrow$):

$$\hat{\mathcal{P}}_{p,q} = c_{\alpha_p, \uparrow}^+ c_{\alpha_q, \downarrow}^+ c_{\alpha_p, \uparrow} c_{\alpha_q, \downarrow}.$$

The spin-up current through electrode a_p can be rewritten in the form

$$I_p = 4\pi^2 \mathcal{N}^2 \sum_q \int d\omega [n_F(\omega - eV) - n_F(\omega)] \gamma_{a_p, \uparrow} \gamma_{a_q, \downarrow} \left| \langle \psi | \hat{\mathcal{P}}_{p,q} | \psi \rangle \right|^2 |G_{x,x,1,2}^A|^2, \quad (36)$$

where $\gamma_{a_{p(q)}, \uparrow} = \pi^2 |t_{a_{p(q)}}|^2 \rho_{a_{p(q)}, \uparrow(\downarrow)}$ denotes the spectral line-width associated to the external electrodes. We first notice that the current is a sum over all possible Cooper pair transmissions, which we already found in section 2. What is new here is that there is one intermediate quantum state involved (the linear superposition). The transport formula can be expressed as suitable projections of this quantum state. These projections correspond to the physical processes by which current is carried away from the quantum state, namely the transport of correlated pairs of electrons. Therefore, the whole picture is consistent: we first identified a wave function, and next showed that transport can be interpreted in terms of quantum measurement of the wave function. In our opinion, the form (36) of the transport formula is not specific to our model, but is valid independently on the microscopic origin of the pairing potential.

This behavior is also consistent with general considerations on decoherence [24, 25, 26, 27], at least on a heuristic basis. I conjecture that there are three distinct stages involved in the decoherence mechanism, which occur on different time scales:

- (A) The initial quantum superposition Eq. 35, being a Schrödinger cat of correlated pairs of electrons.
- (B) An intermediate stage in which the Schrödinger cat superposition is lost but there are still pair correlations. Namely, the spin-up (-down) electrons have tunneled into the specific reservoirs p (q). The correlated pair still behaves like a two-electron phase coherent object.
- (C) The final stage in which the two electrons making the correlated pair behave like independent quasi-particles, with no more pair correlations.

The transition (B) \rightarrow (C) is usually known as the proximity effect. I conjecture that the projector appearing in Eq. 36 is the signature of the decoherence process (A) \rightarrow (B). Note that because two-electron correlations are preserved until stage (C), there is an interesting physics going on at stage (B) which is explored in the next section.

The reader might object that the intermediate regions may contain thousands of electrons. It may then appear counter-intuitive to propose Schrödinger cat made of superpositions of a large number of electrons. This is certainly true, and one should keep in mind that *the wave function Eq. 35 is by no way the many body ground state wave function*. Instead it is intended to describe only the degrees of freedom that participate to transport.

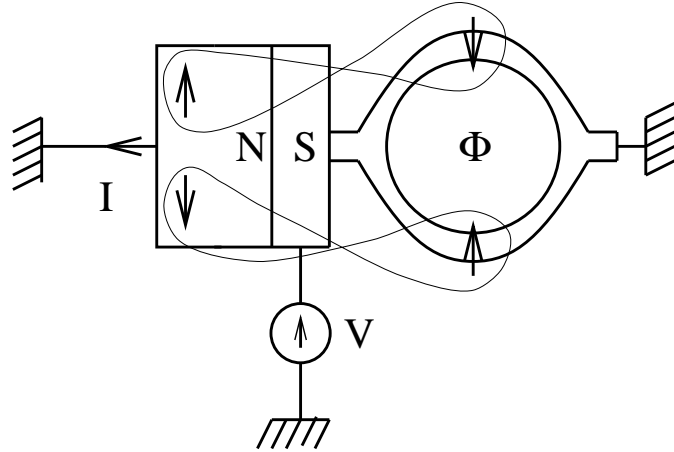


Figure 10: Geometry of the Aharonov-Bohm experiment. The current I flowing into the left electrode is modulated by the flux enclosed by the other electron making the correlated pair. The non separable correlations between the left electrode and the Aharonov-Bohm loop are represented schematically.

5 Aharonov-Bohm effect

Now I propose a device that can be used to probe non separable correlations. For this purpose, I consider the geometry on Fig. 10, in which one side of the superconductor is connected to an Aharonov-Bohm loop (being made of a normal metal), while the other side is connected to a normal metal that does not contain any hole. I show that the current flowing through the electrode with no hole is modulated by the flux enclosed by the normal metal loop. This means that the current due to one electron making a correlated pair is modulated by the flux enclosed by the other electron, which is a manifestation of non separable correlations. The electrodes are considered to be normal metals in which phase coherence can propagate over large distances.

I consider the circuit on Fig. 11 that is used to model the situation on Fig. 10. The hopping parameters are complex number, for instance $t_{a,a'} = t \exp(i\varphi_{a,a'}) = t \exp[2i\pi\phi/(4\phi_0)]$, and $t_{a',a} = t \exp(i\varphi_{a',a}) = t \exp[-2i\pi\phi/(4\phi_0)]$. Since I use effective single site Green's functions in which a' and a'' are represented by the same single site, this choice of the hopping insures that $\oint \varphi_{i,j} = 2\pi\phi/\phi_0$. The first task is to solve the chain of Dyson equations

$$G_{a,a} = g_{a,a} + g_{a,a}t_{a,a'}G_{a',a} + g_{a,a}t_{a,a''}G_{a'',a} \quad (37)$$

$$G_{a',a} = g_{a',a'}t_{a',a}G_{a,a} + g_{a',b'}t_{b',b}G_{b,a} \quad (38)$$

$$G_{a'',a} = g_{a'',a''}t_{a'',a}G_{a,a} + g_{a'',b''}t_{b'',b}G_{b,a} \quad (39)$$

$$G_{b,a} = g_{b,b}t_{b,b'}G_{b',a} + g_{b,b}t_{b,b''}G_{b'',a} \quad (40)$$

$$G_{b',a} = g_{b',b'}t_{b',b}G_{b,a} + g_{b',a'}t_{a',a}G_{a,a} \quad (41)$$

$$G_{b'',a} = g_{b'',b''}t_{b'',b}G_{b,a} + g_{b'',a''}t_{a'',a}G_{a,a}. \quad (42)$$

Next we need to calculate the Keldysh component

$$G_{a,a}^{+-} = [1 + G_{a,a}^R t_{a',a} + G_{a,a''}^R t_{a'',a}] g_{a,a}^{+-} [1 + t_{a,a'} G_{a',a}^A + t_{a,a''} G_{a'',a}^A] \quad (43)$$

$$+ [G_{a,b''}^R t_{b'',b} + G_{a,b'}^R t_{b',b}] g_{b,b}^{+-} [t_{b,b'} G_{b',a}^A + t_{b,b''} G_{b'',a}^A] \quad (44)$$

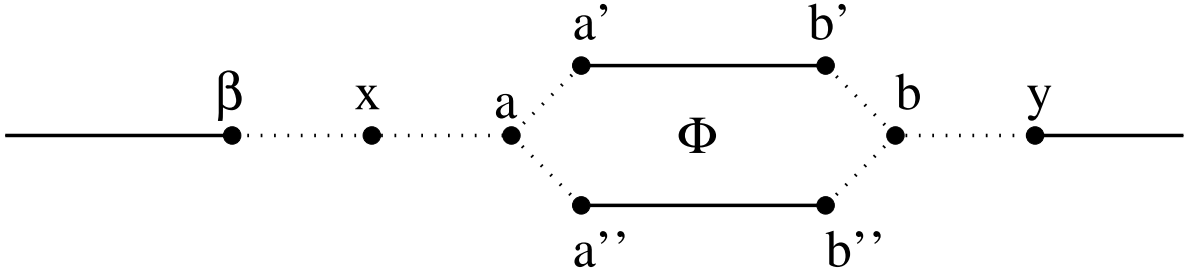


Figure 11: The circuit used to represent the situation on Fig. 10. x is superconducting, β is ferromagnetic and the remaining sites are normal metals.

$$+ G_{a,a}^R t_{a,a'} g_{a',a'}^{+-} t_{a',a} G_{a,a}^A \quad (45)$$

$$+ G_{a,a}^R t_{a,a''} g_{a'',a''}^{+-} t_{a'',a} G_{a,a}^A \quad (46)$$

$$+ G_{a,a}^R t_{a,a'} g_{a',b'}^{+-} t_{b',b} G_{b,a}^A \quad (47)$$

$$+ G_{a,b}^R t_{b,b'} g_{b',a'}^{+-} t_{a',a} G_{a,a}^A \quad (48)$$

$$+ G_{a,a}^R t_{a,a''} g_{a'',b'}^{+-} t_{b',b} G_{b,a}^A \quad (49)$$

$$+ G_{a,b}^R t_{b,b''} g_{b'',a''}^{+-} t_{a'',a} G_{a,a}^A \quad (50)$$

$$+ G_{a,b}^R t_{b,b'} g_{b',b'}^{+-} t_{b',b} G_{b,a}^A \quad (51)$$

$$+ G_{a,b}^R t_{b,b''} g_{b'',b''}^{+-} t_{b'',b} G_{b,a}^A. \quad (52)$$

One finds $G_{a,a}^{A,R} = \pm i\pi\tilde{\rho}_a$, and $G_{a,a}^{+-} = 2i\pi n_F(\omega)\tilde{\rho}_a$, with the renormalized density of states

$$\tilde{\rho}_a = \frac{\rho_a [1 + \rho_b(\gamma' + \gamma'')]}{1 + (\rho_a + \rho_b)(\gamma' + \gamma'') + 2\gamma'\gamma''\rho_a\rho_b [1 - \cos(2\pi\phi/\phi_0)]}, \quad (53)$$

and where I used the notation $\gamma' = \pi^2 t^2 \rho'$ and $\gamma'' = \pi^2 t^2 \rho''$ with $t = |t_{a,a'}| = |t_{a,a''}| = |t_{b,b'}| = |t_{b,b''}|$.

It is straightforward to use the same procedure as in section 4.3 to eliminate disconnected processes, which leads to $I_\beta^A = I_{\beta,\text{local}}^A + I_{\beta,\uparrow,\text{nonlocal}}^A + I_{\beta,\downarrow,\text{nonlocal}}^A$, where the local contribution takes the form

$$I_{\beta,\text{local}}^A = 4\pi^2 |t_{x,\beta}|^4 \rho_{\beta,\uparrow} \rho_{\beta,\downarrow} \int d\omega [n_F(\omega - eV) - n_F(\omega)] |G_{x,x,1,2}^A|^2, \quad (54)$$

and the non local contribution is

$$I_{\beta,\sigma,\text{nonlocal}}^A = \int d\omega \hat{Q} \left[\frac{4\pi^2 |t_{x,\beta}|^2 |t_{x,a}|^2 \rho_{\beta,\sigma} \rho_{a,-\sigma}^2 \rho_{b,-\sigma}^2 [(\gamma'_{-\sigma} + \gamma''_{-\sigma})^2 + 2\gamma'_{-\sigma} \gamma''_{-\sigma} [1 - \cos(2\pi\phi/\phi_0)]]}{[1 + (\rho_{a,-\sigma} + \rho_{b,-\sigma})(\gamma'_{-\sigma} + \gamma''_{-\sigma}) + 2\gamma'_{-\sigma} \gamma''_{-\sigma} \rho_{a,-\sigma} \rho_{b,-\sigma} [1 - \cos(2\pi\phi/\phi_0)]]^2} \right] \times [n_F(\omega - eV) - n_F(\omega)] |G_{x,x,1,2}^A|^2, \quad (55)$$

where the action of \hat{Q} has already been given. The non local current Eq. 55 is periodic in ϕ/ϕ_0 . Such oscillations are a signature of non separable correlations.

The origin of these oscillations can be understood in simple terms in the limit $t_{a,x}, t_{b,y} \ll 1$, where the physics is the one of resonant tunneling. There are discrete energy levels on the loop, the energy of which depends on the magnetic flux. Single electron transmission is modulated by the flux because the transmission is larger when there is one resonant level. Now the Andreev current is carried by

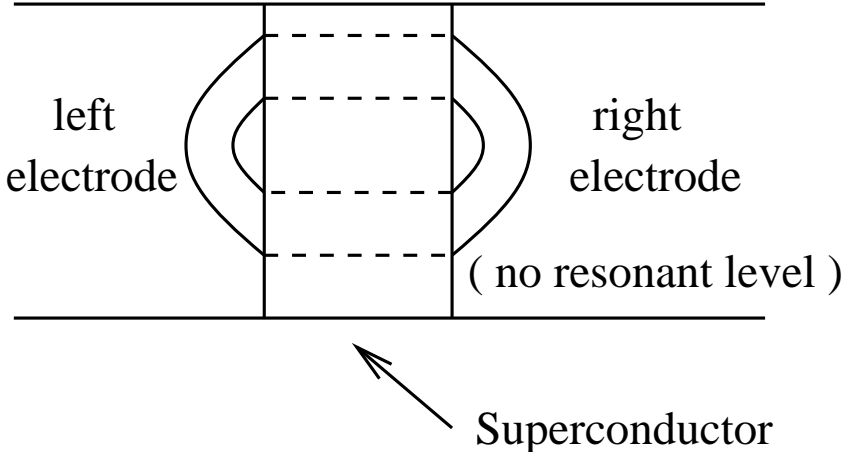


Figure 12: The diagram involved in the absence of resonant tunneling in the right electrode. This diagram does not carry electrical charge.

correlated pairs of electrons. If the Aharonov-Bohm loop is off-resonance, one electron making the correlated pair (for instance a spin-up electron) cannot be transmitted. As a consequence, the whole correlated pair cannot be transmitted. There is therefore no spin-down current.

This situation is not far from the behavior of the multichannel ferromagnet – superconductor junction. It is well known that in such junctions there is no current transmitted in the channels having only a spin-up Fermi surface [28].

The following equivalent explanation can be found. There is one virtual state in which one Cooper pair has been extracted from the superconductor, one electron is in the left electrode and the other electron is in the right electrode. Since there is no resonant level, the electron in the right electrode is backscattered onto the superconductor, undergoes an Andreev reflection in which one Cooper pair is transferred into the superconductor, and a hole is transferred in the left electrode. The whole processes is represented on Fig. 12. A quick look at this diagram shows that there is no current transmitted. Note that the processes involved in the multichannel superconductor – ferromagnet junction can be interpreted with the same diagram [29].

We stress that these two pictures based on resonant tunneling hold only if the interfaces have low transparency contacts. Nevertheless, since we found a systematic way to handle higher order Feynman diagram, the model is valid also for high transparency contacts, in which case Aharonov-Bohm oscillations are also predicted.

6 Propagation of superconducting correlations along a domain wall

Now, I illustrate the consequence of the model regarding the propagation of superconducting correlations along domain walls in ferromagnets. Such propagation can generate an enhancement of the proximity effect in ferromagnet / superconductor heterostructures, not against recent experiments [13, 14, 15, 30]. We use the geometry on Fig. 13 to address this problem in an effective single site formalism. If site α has a spin-up orientation and site β has a spin-down orientation, there is one domain wall in the junction. In the presence of partially polarized ferromagnets, a spin- σ electron can be transferred across the domain wall because of the hopping matrix element t' . This provides a minimal model for Cooper pair penetration along domain walls. This model in which the domain

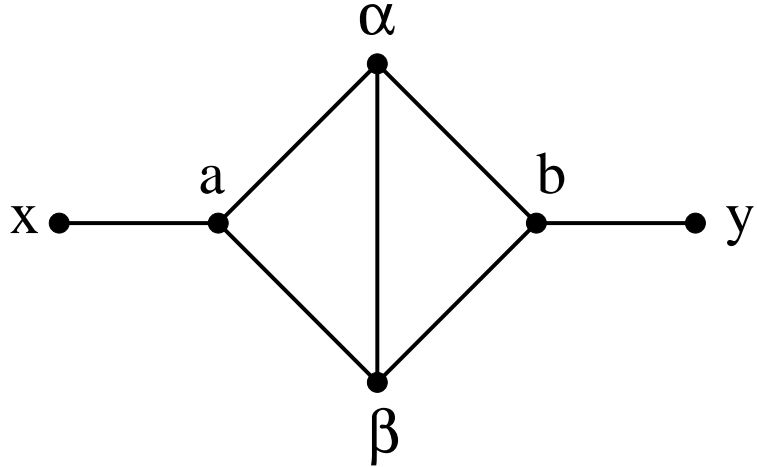


Figure 13: The circuit used to represent the propagation of superconducting correlations along a domain wall. There is a domain wall if α has a spin-up magnetization and β has a spin-down magnetization. I note $t = t_{a,\alpha} = t_{a,\beta} = t_{b,\alpha} = t_{b,\beta}$ and $t' = t_{\alpha,\beta}$. Site x is superconducting.

wall has a vanishing width is expected to be relevant for describing a situation in which the width of the domain wall is smaller than the superconducting coherence length.

The Dyson equations corresponding to Fig. 13 take the form

$$G_{a,a} = g_{a,a} + g_{a,a}t_{a,\alpha}G_{\alpha,a} + g_{a,a}t_{a,\beta}G_{\beta,a} \quad (56)$$

$$G_{\alpha,a} = g_{\alpha,\alpha}t_{\alpha,a}G_{a,a} + g_{\alpha,\alpha}t_{\alpha,\beta}G_{\beta,a} + g_{\alpha,\alpha}T_{\alpha,b}G_{b,a} \quad (57)$$

$$G_{\beta,a} = g_{\beta,\beta}t_{\beta,a}G_{a,a} + g_{\beta,\beta}t_{\beta,\alpha}G_{\alpha,a} + g_{\beta,\beta}t_{\beta,b}G_{b,a} \quad (58)$$

$$G_{b,a} = g_{b,b}t_{b,\alpha}G_{\alpha,a} + g_{b,b}t_{b,\beta}G_{\beta,a}, \quad (59)$$

and similar equations hold for the Keldysh component. These equations are solved into $G_{a,a}^{A,R} = \pm i\pi\tilde{\rho}_a$, $G_{a,a}^{+-} = 2i\pi n_F(\omega)\tilde{\rho}_a$, with the renormalized density of states

$$\tilde{\rho}_a = \rho_a \frac{1 + \pi^2 t'^2 \rho_\alpha \rho_\beta + \pi^2 t^2 \rho_b [\rho_\alpha + \rho_\beta + 2i\pi t' \rho_\alpha \rho_\beta]}{1 + \pi^2 t'^2 \rho_\alpha \rho_\beta + \pi^2 t^2 (\rho_a + \rho_b) [\rho_\alpha + \rho_\beta + 2i\pi t' \rho_\alpha \rho_\beta]}. \quad (60)$$

I deduce from Eq. 60 that the Andreev reflection current takes the form

$$I^A = 4\pi^6 t_{a,\alpha}^4 t^8 \int d\omega \hat{Q} \left[\prod_{\sigma=\uparrow,\downarrow} \frac{\rho_{x,\sigma} \rho_{a,\sigma}^2 \rho_{b,\sigma} \left[(\rho_{\alpha,\sigma} + \rho_{\beta,\sigma})^2 + 4\pi^2 t'^2 \rho_{\alpha,\sigma}^2 \rho_{\beta,\sigma}^2 \right]}{|1 + \pi^2 t'^2 \rho_{\alpha,\sigma} \rho_{\beta,\sigma} + \pi^2 t^2 [\rho_{\alpha,\sigma} + \rho_{\beta,\sigma} + 2i\pi t' \rho_{\alpha,\sigma} \rho_{\beta,\sigma}]|^2} \right] \times \quad (61)$$

$$[n_F(\omega - eV) - n_F(\omega)] |G_{x,x,1,2}^A|^2. \quad (62)$$

In the limit of fully polarized ferromagnets, the current Eqs. 61, 62 vanishes if the sites α and β have the same spin orientation. In the presence of a domain wall, α and β have an opposite spin orientation, in which case Cooper pairs can be transferred across the junction even in the presence of fully polarized ferromagnets.

The effect proposed here is related to two other well known problems:

- (i) *The π -junction:* It is well known that Cooper pairs cannot propagate over large distances in a ferromagnetic metal. In fact, they cannot even propagate at all in a fully polarized single domain

ferromagnet. In partially polarized ferromagnets, Cooper pair penetration gives rise to the π -junction physics that has been investigated by theorists since several decades [31, 32, 33, 34], and has been obtained experimentally only recently [35, 36]. We have shown here that Cooper pairs can propagate in fully spin polarized ferromagnets if there are domain walls in the ferromagnet. The number of conduction channels is equal to the number of domain walls.

- (ii) *Cryptomagnetism*: It has been established a long time ago by Anderson and Suhl that ferromagnetism and superconductivity can accommodate each other in the same system if the ferromagnet acquires a domain structure [37, 38]. Our proposal can be viewed as the proximity effect version of cryptomagnetism.

7 Conclusion

To conclude, I have provided a minimal formalism to treat non separable correlations generated when a superconductor is in contact with ferromagnetic or normal metal electrodes. It has been shown how to solve the problem of disconnected contributions arising in this formalism, and it has been given a systematic way to handle the infinite series of Feynman diagram.

We answered the four questions given in the introductory section, namely:

- (i) The superconducting gap depends on the relative spin orientation of ferromagnetic electrodes connected to a superconductor. This might be probed in experiments.
- (ii) It is possible to fabricate linear superpositions of correlated pairs of electrons. Transport in these systems can be expressed in terms of projections of the linear superposition of correlated pairs of electrons. The wave function is projected on the relevant quantities that participate to transport, *i.e.* the correlated pairs of electrons.
- (iii) I proposed a new Aharonov-Bohm experiment to test non separable correlations. In this experiment, the spin- σ electron making the Cooper is forced to couple to a magnetic flux while the spin- $(-\sigma)$ electron has an ordinary propagation. It has been shown that the spin- σ current oscillates as a function of the magnetic flux coupled to the spin-down electron. It has been predicted that the effect appears with low and high transparency contacts, and independently of the spin polarization of the electrodes. Therefore, normal metal electrodes can be used, in which phase coherence can propagate over large distances.
- (iv) It has been shown that superconducting correlations can propagate along ferromagnetic domain walls. The model is strictly speaking valid if the width of the domain wall is small but we are confident about forthcoming generalizations of the model. The number of Cooper pair conduction channels is equal to the number of domain walls. This may apply to existing experiments in heterostructures [13, 14, 15] which have not received a satisfactory explanation up to now in spite of various theoretical attempts [15, 30].

To end-up let us mention that the work presented in this article calls both for new experiments and for more sophisticated theoretical descriptions. It is in general needed to incorporate realistic ingredients in the models, which will be the subject of future publications. Nevertheless, we have no doubt that the same physics will be obtained in the presence of realistic constraints.

The author acknowledges fruitful discussions with P. Degiovanni, D. Feinberg and M. Giroud. This work is supported by the French Ministry of Research under contract ACI 2086 CDR2.

References

- [1] P.W. Schor, in *Proc. 35th Symposium on the Foundations of Computer Science* (IEEE Computer Society Press), 124 (1994).
- [2] L.K. Grover, *Phys. Rev. Lett.* **79**, 325 (1997).
- [3] A. Steane, *Rep. Prog. Phys.* **61**, 117 (1998).
- [4] Y. Nakamura, Yu. A. Pashkin, and J.S. Tsai, *Nature* **398**, 786 (1999).
- [5] D. Loss and E.V. Sukhorukov, *Phys. Rev. Lett.* **84**, 1035 (2000).
- [6] O. Buisson and F.W.J. Hekking, arXiv:cond-mat/0008275.
- [7] J.S. Bell, *Physics (N.Y.)* **1**, 195 (1965).
- [8] A. Aspect, P. Grangier, and G. Roger, *Phys. Rev. Lett.* **47**, 460 (1981);
A. Aspect, J. Dalibard, and G. Roger, *ibid.* **49**, 1904 (1982).
- [9] P.G. Kwiat *et al.*, *Phys. Rev. Lett.* **75**, 4337 (1995).
- [10] G.B. Lesovik, T. Martin, and G. Blatter, arXiv:cond-mat/0009193.
- [11] G. Deutscher and D. Feinberg, *App. Phys. Lett.* **76**, 487 (2000).
- [12] G. Falci, D. Feinberg, and F.W.J. Hekking, *Europhysics Letters* to appear, arXiv:cond-mat/0011339.
- [13] M. Giroud *et al.*, *Phys. Rev. B* **58**, R11872 (1998).
- [14] V.T. Petrashov, I.A. Sosnin, and C. Troadec, arXiv:cond-mat/0007278.
- [15] J. Aumentado and V. Chandrasekhar, arXiv:cond-mat/0007433.
- [16] Y. Aharonov and D. Bohm, *Phys. Rev.* **115**, 125 (1959).
- [17] M. Büttiker, Y. Imry and R. Landauer, *Phys. Lett.* **96 A**, 365 (1983).
- [18] R.A. Webb and S. Washburn, *Physics Today*, December 1998, and references therein.
- [19] Y. Aharonov and A. Casher, *Phys. Rev. Lett.* **53**, 319 (1984).
- [20] M. Tinkham, *Introduction to superconductivity*, Mc Graw-Hill, N.Y. (1996).
- [21] A. Martin-Rodeiro, F.J. Garcia-Vidal, and A. Levy-Yeyati, *Phys. Rev. Lett.* **72**, 554 (1994).
J.C. Cuevas, A. Martin-Rodero, and A. Levy Yeyati, *Phys. Rev. B* **54**, 7366 (1996).
- [22] C. Caroli, R. Combescot, P. Nozières and D. Saint-James, *J. Phys. C: Solid St. Phys.* **4**, 916 (1971).
- [23] A. Einstein, B. Podolsky, and N. Rosen, *Phys. Rev.* **47**, 777 (1935).
D. Bohm and Y. Aharonov, *Phys. Rev.* **108**, 1070 (1957).

- [24] W. Unruh and W. Zurek Phys. Rev. **D 40**, 1071 (1989).
- [25] W. Zurek, Phys. Rev. **D 26**, 1862 (1982).
- [26] W. Zurek, Physics Today **44**, 36 (1991).
- [27] P. Degiovanni and S. Peysson, Phys. Rev. B **62**, 10706 (2000).
- [28] M.J.M. de Jong and C.W.J. Beenakker, Phys. Rev. Lett. **74**, 1657 (1995).
- [29] R. Mélin, Europhysics Letters **51**, 202 (2000).
- [30] W. Belzig, A. Brataas, Yu. V. Nazarov, and G.E. Bauer, arXiv:cond-mat/0005188.
- [31] P. Fulde and A. Ferrel, Phys. Rev. **135**, A550 (1964).
- [32] A. Larkin and Y. Ovchinnikov, Sov. Phys. JETP **20**, 762 (1965).
- [33] M. A. Clogston, Phys. Rev. Lett. **9**, 266 (1962).
- [34] E.A. Demler, G.B. Arnold and M.R. Beasley, Phys. Rev. B **55**, 15174 (1997).
- [35] V.V. Ryazanov *et al.*, arXiv:cond-mat/0008364
- [36] T. Kontos, M. Aprili, J. Lesueur and X. Grison, arXiv:cond-mat/0009192.
- [37] P. Anderson and H. Suhl, Phys. Rev. **116**, 6739 (1959).
- [38] A. Buzdin and L. Bulaevskii, JETP **67**, 576 (1988).